ELSEVIER

Carbohydrate Research 297 (1997) 309–324

CARBOHYDRATE RESEARCH

Automated docking of isomaltose analogues in the glucoamylase active site

Pedro M. Coutinho [a], Michael K. Dowd [b], Peter J. Reilly [a,*]

[a] *Department of Chemical Engineering, Iowa State University, Ames, IA 50011, USA*
[b] *Southern Regional Research Center, U.S. Department of Agriculture, New Orleans, LA 70179, USA*

Received 15 July 1996; accepted 14 October 1996

Abstract

Low-energy conformers of analogues of the disaccharide isomaltose were determined with MM3(92) and were then flexibly docked into the glucoamylase active site using AutoDock 2.1. This procedure has produced bound complexes of saccharides with glucoamylase comparable to those obtained by protein crystallography. Conformational energy surfaces of three methyl α-isomaltosides, two with a second methyl group at C-6_B, were determined to characterize the steric limitations introduced by that group. Their most probable conformers were used as initial structures for docking. Seven sets of monodeoxy methyl α-isomaltoside structures were also generated based on the methyl α-isomaltoside conformational map and were docked to probe the contribution of individual hydroxyl groups to binding. The optimized docking modes are similar for most analogues, and energies of intermolecular interaction per extended atom agree with the assignment of key hydroxyl groups made from kinetic studies. This new approach to study saccharide–protein interactions complements the results of protein crystallography, allowing a better understanding of the interaction of glucoamylase with its substrates.

Keywords: AutoDock; Docking; Glucoamylase; Isomaltose; MM3; Molecular mechanics; Simulated annealing

1. Introduction

Glucoamylase [α-(1 → 4)-D-glucan glucohydrolase, EC 3.2.1.3, GA] hydrolyzes terminal α-(1 → 4)-D-glycosidic bonds from the nonreducing ends of maltooligosaccharides to produce β-D-glucose, and is used industrially to digest liquefied starch. Its ability to hydrolyze α,β-(1 → 1)-, α-(1 → 2)-, α-(1 → 3)-, and α-(1 → 6)-D-glycosidic bonds [1] can lead at high D-glucose concentrations to the formation of different condensation products [2,3]. Among these, the disaccharide isomaltose and the trisaccharides isomaltotriose and panose, which contain α-(1 → 6)-D-glucosidic linkages, are thermodynamically favored. Reduction of the yield of these compounds by protein engineering requires understanding of GA selectivity at the molecular level.

The structure of the *Aspergillus awamori* var. *X100* GA catalytic domain has been obtained by X-ray crystallography under different pH conditions

* Corresponding author. Tel.: +1-515-294-5968; Fax: +1-515-294-2689; E-mail: reilly@iastate.edu.

0008-6215/97/$17.00
PII S0008-6215(96)00283-2

and while complexed to different inhibitors [4–9]. The GA active site, a well in the center of an $(\alpha/\alpha)_6$ barrel, is rigid under these different conditions. The two catalytic residues, the acid Glu179 and the base Glu400 [5,10,11], are found at opposite sides of the active-site cavity that also encloses the putative catalytic water molecule [5]. Other essential residues, conserved in fungal, yeast, and bacterial GAs where they constitute the active-site walls, are equally important in catalysis [12–14].

Seven and six subsites have been found in the *A. awamori / Aspergillus niger* GA active site through kinetic measurements of malto- [15–17] and isomalto-oligosaccharide [16] hydrolysis, respectively. The positions of maltooligosaccharide residues in the first four subsites can be defined from crystallographic data for the acarbose and *gluco*-dihydroacarbose GA complexes [7–9], two alternative positions for the third and fourth subsites being found [8,9]. Unfortunately, no crystallographic data exist for α-(1 → 6)-linked substrate analogues complexed with GA. 6^2-Thiopanose and different 6^{ω}-*S*-α-D-glucopyranosyl-6^{ω}-thiomaltooligosaccharides, containing α-(1 → 6) thioglucosidic linkages at their nonreducing ends, have limited, if any, interaction with the GA catalytic domain [18,19]. Only recently, a pseudo-disaccharide derived from isofagomine that is analogous to an α-(1 → 6)-linked disaccharide has been reported as a strong GA inhibitor [20].

Conformational studies have shown that isomaltose is a very flexible disaccharide [21], since three-bond α-(1 → 6) glycosidic linkages contribute to a reduced interaction between disaccharide pyranosyl rings [21,22]. However, inter-ring torsional potentials yielded fairly sharp minima. A limited conformational search on the transition-state complex of isomaltose with GA showed that the GA active site can accommodate this substrate [23], with the critical OH-4_A, OH-6_A, and OH-4_B groups of isomaltose [24] taking the position of the critical OH-4_A, OH-6_A, and OH-3_B groups of maltose [25] as taken from the GA–acarbose complex [6]. Kinetic studies with conformationally biased isomaltose analogues [26,27] suggested that the preferred conformations of methyl α-isomaltosides (MIs) are important in GA hydrolysis.

The role of individual substrate hydroxyl groups in GA catalysis has been explored kinetically for isomaltose [23,24] as well as for maltose [25,28,29]. Key saccharide hydroxyl groups not only provide the complementary structure required for protein binding through hydrogen bonding [30,31], but they also establish essential polar interactions to anchor the substrate in the enzyme active site and to induce catalysis [32].

Monte Carlo methods can be used for automated docking of flexible substrates to proteins by simulated annealing [33–35]. A new combined molecular mechanics/simulated annealing approach recently yielded GA interactions with monosaccharide substrates and mono- and di-saccharide analogues that closely matched results obtained by X-ray crystallography [36]. Individual docking of the most significant conformers of three different forms of methyl α-acarviosinide allowed the exploration of their interactions with the active site. Upon redocking, which entailed the optimization of the original docking results by repetition of the docking protocol, the active-site conformations were similar to the experimentally determined conformations of the nonreducing end of the inhibitor acarbose in the *A. awamori* var. *X100* GA–acarbose complex [6].

In this study, ten different methyl α-isomaltosides were docked in the *A. awamori* var. *X100* GA active site by simulated annealing with AutoDock 2.1. This was preceded by conformational analysis using MM3(92) of MI and of two conformationally biased analogues, methyl 6R-C-MI and methyl 6S-C-MI, to select low-energy conformations of each compound for docking. A systematic study of the structural interaction of monodeoxy MIs with GA was performed to assess the role of individual hydroxyl groups in binding and catalysis.

2. Computational methods

Conformational analysis of methyl α-isomaltosides.—The MM3(92) force field [37–39], obtained from Technical Utilization Corporation, Powell, OH, but now available from Quantum Chemistry Program Exchange (QCPE), Bloomington, IN, was used in this study. As in previous disaccharide conformational studies [21,22,40–43], the bulk dielectric constant (e) was set to 4.0. Starting structures of MI and of the conformationally biased methyl 6R-C-MI and methyl 6S-C-MI (Fig. 1) were generated and preoptimized using PC-Model (Serena Software, Bloomington, IN). Eight sets of exo-cyclic orientations were considered for each disaccharide. These were all combinations of clockwise (c) and reverse-clockwise (r) orientations of the secondary hydroxyl groups for each ring, where partial crowns of weak hydrogen bonds tend to be formed in vacuum and to a lesser

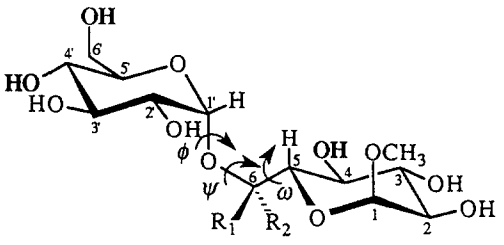

Fig. 1. MI (R_1 = H; R_2 = H), methyl 6R-C-MI (R_1 = CH_3; R_2 = H), and methyl 6S-C-MI (R_1 = H; R_2 = CH_3) with angles ϕ, ψ, and ω denoted. The critical hydroxyl groups required for isomaltose hydrolysis are shown in bold [27].

extent in crystals and solution [44]. For the C-5_A–C-6_A bond, orientations *gauche* to both C-4_A and O-5_A, referred to as *gauche–gauche* (*gg*), and *gauche* to O-5_A and *trans* to C-4_A, referred to as *gauche-trans* (*gt*), where considered, since these are favored by glucopyranosyl rings in both solution and in crystals [45–47].

The torsional angles of the rings about the glucosidic linkage were defined as $\phi = \Theta$(H-1_A–C-1_A–O-6_B–C-6_B), $\psi = \Theta$(C-1_A–O-6_B–C-6_B–C-5_B), and $\omega = \Theta$(O-6_B–C-6_B–C-5_B–H-5_B), where A and B represent the non-reducing and reducing end glycosyl units, respectively (Fig. 1). The conformational space for the three linkage torsional angles was evaluated with MM3(92) at 20° intervals, relaxing all remaining geometric features. The lowest energy value at each grid point from the different sets was used to draw contour maps with Surfer (Golden Software, Golden, CO) and three-dimensional isoenergy surfaces using Dicer (Fortner Research LLC, Sterling, VA).

Local minima were found by a multistep procedure where all starting structures that could contribute to a local minimum were rotated to a local low-energy grid point, optimized there, and then reoptimized without torsional angle restrictions using the full-matrix option of MM3. The lowest energy structure was taken as the minimum. Local minima within 8 kcal/mol of the global minimum were used as initial starting structures for docking.

Structures of 2′-, 3′-, 4′-, 6′-, 2-, 3-, and 4-deoxy MI were generated using the procedure described above. Since no significant conformational differences were expected between MI and its monodeoxy analogues, conformers were generated for each analogue by rotating the glycosidic dihedrals to the values found in each of the MI minima, optimizing the structures there, and finally reoptimizing without restrictions.

Docking simulations.—Automated docking simulations were conducted with AutoDock 2.1 [33–35] (Scripps Research Institute, La Jolla, CA). The GA crystal structure as in the complex with D-*gluco*-dihydroacarbose [8,9] (Brookhaven Protein Databank entry 1GAI) was used. The inhibitor and all water molecules except the putative catalytic molecule were removed, and nonpolar hydrogens were added using Quanta 3.3 (Molecular Simulations, Inc., San Diego, CA). Atomic partial charges for GA and ligands were calculated by the Gasteiger method [48].

Atomic interaction energy grids were calculated using probes corresponding to each atom type found in the substrate, at 0.5 Å grid positions in a 40 Å cubic box centered on the GA active site. The electrostatic interaction energy grid used a sigmoidal distance-dependent dielectric function [49] to account for the solvent screening effect. The Lennard–Jones coefficients of AutoDock 1.0 with different parameters for apolar and polar hydrogens were used, along with a distance criterion with directional attenuation to account for hydrogen bonding.

At the start of each docking study, the nonreducing end ring of each substrate was placed in the active site. Each docking experiment consisted of 100 independent Monte Carlo simulations per starting structure. As in the previous study [36], a short schedule [34] with 100 constant-temperature cycles was used. Each cycle had a maximum of 1500 steps accepted or rejected, the minimal energy structure being passed to the next cycle. The temperature was reduced by a 0.95 factor per cycle from an initial value of T = 50.33 K (or RT = 100 cal/mol), and the maximal torsional rotation per step was reduced by a factor of 0.9875 per cycle from the initial 15°. A constant maximal translational step of 0.2 Å per step was used. All disaccharide exocyclic and inter-ring dihedral angles were allowed to rotate.

Docking simulations were made for each of seven MI, seven methyl 6R-C-MI, and six methyl 6S-C-MI conformers having local minima 8 kcal/mol or less above their respective global minima given by MM3(92). For each monodeoxy MI, seven different conformers generated from the equivalent MI conformers were used as initial structures in docking simulations.

Following docking, all structures generated for a single compound were subjected to cluster analysis, cluster families being based on a tolerance of 1 Å for an all-atom root-mean-square (RMS) deviation from an optimal structure. For each substrate, the global

minimum structure, optimal structures of significant clusters, and occasionally other significant structures were subjected to redocking and cluster analysis. Redocking, or repetition of the docking protocol using a previously obtained result [36], allows an economic and efficient use of the short protocol [34] where only promising structures of the many initial docking results are further optimized. All results were compared to the best result for MI. To obtain consistent results of substrate internal energies among all experiments, only AutoDock's (AD) variation on internal energy was considered as before [36], all values being referenced to the MM3(92) relative energy:

$$\underset{\text{(Docking)}}{\text{Internal Energy}} = \text{Relative MM3 Energy} + \Delta[\underset{\text{(Docking)}}{\text{AD Internal Energy}}]$$

$$\underset{\text{(Redocking)}}{\text{Internal Energy}} = \underset{\text{(Docking)}}{\text{Internal Energy}} + \Delta[\underset{\text{(Redocking)}}{\text{AD Internal Energy}}]$$

3. Results and discussion

Conformational analysis of methyl α-isomaltosides.—Isoenergy surfaces 2, 4, 6, and 8 kcal/mol above their global minima are shown in Figs. 2–4 for MI, methyl 6R-C-MI, and methyl 6S-C-MI, respectively. Six corresponding contour plots for the staggered and eclipsed orientations of ω of each compound are shown in Figs. 5–7. Local minima within the lowest 8 kcal/mol of the global minima of the three MIs appear in Table 1. Conforming to the *exo*-anomeric effect, all minima have ϕ values between $-18°$ and $-46°$ except the seventh minimum of methyl 6R-C-MI. The results for MI are very similar to those obtained for α-isomaltose [21], the order of the energetically close first two minima being reversed. The extra methyl groups of the methyl 6-C-MIs cause a negative and a positive deviation of φ in the several minima of the *R*- and *S*-isomers, respectively, constraining the available conformational space differently. For methyl 6R-C-MI all staggered orientations of ω (Fig. 6b,d,f) are slightly constrained compared to MI (Fig. 5b,d,f) but the

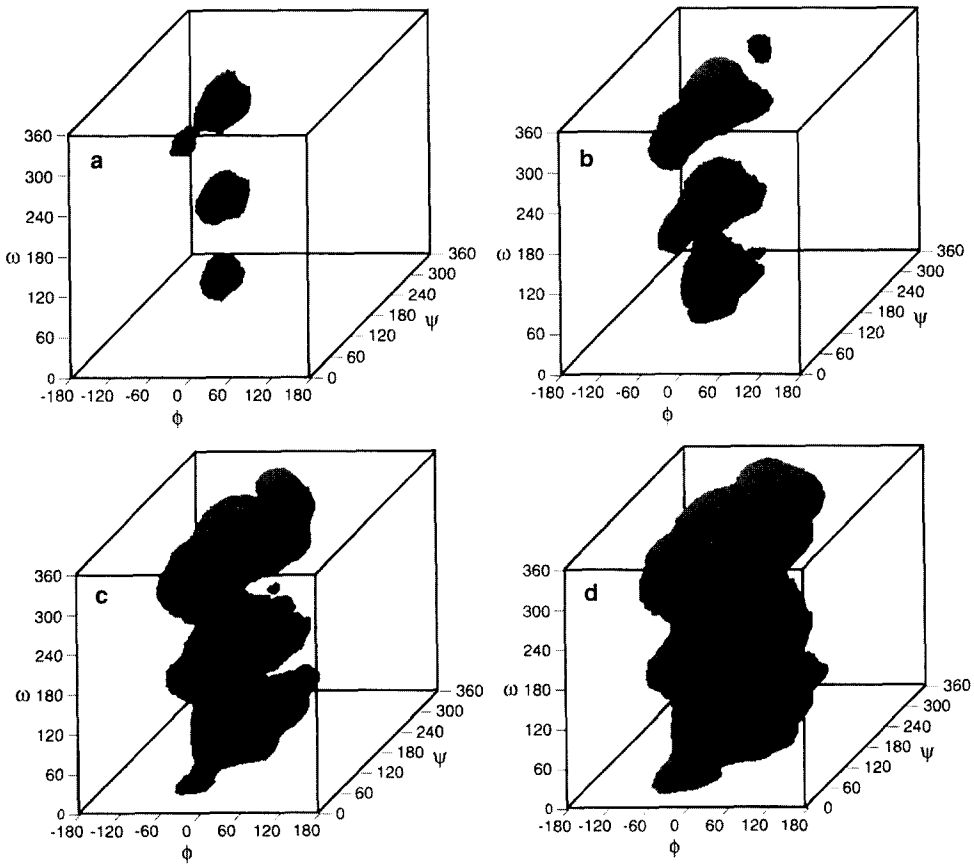

Fig. 2. MM3(92)-generated isoenergy surfaces for MI: (a) 2 kcal/mol, (b) 4 kcal/mol, (c) 6 kcal/mol, and (d) 8 kcal/mol. For ease of viewing, the ϕ axis runs from $-180°$ to 180° and the ψ and ω axes run from 0° to 360°.

eclipsed orientation at $\omega = -120°$ (Fig. 6e) is especially constrained, as seen in the relaxed-residue energy surfaces (Fig. 3). For methyl 6S-C-MI the staggered orientations of ω (Fig. 7b,d,f) are even more constrained, with a stronger impairment of movement in all eclipsed orientations of ω (Fig. 7a,c,e), limiting the movement to the spatial regions close to the different minima (Fig. 4).

For methyl 6R-C-MI in solution, the set $\phi/\psi/\omega = -50°/90°/-60°$ estimated by NMR [26] corresponds to the values obtained for the second minimum by MM3. Likewise, for methyl 6S-C-MI the NMR set $\phi/\psi/\omega = -50°/-165°/180°$ [26] is very close to the conformation of the global minimum.

Docking of methyl α-isomaltosides.—Following docking (data not shown) the optimal, or lowest energy, structures of the energetically significant clusters and some others were redocked. Significant clusters of redocked MIs are listed in Table 2. The optimal structures of the different MIs are *gg* conformers except for a *gt* conformer of MI. However, the optimal *gg* structure of MI, representing the second cluster, is close to the *gt* conformer in total interaction energy. The *gg* or equivalent conformation of the exocyclic hydroxymethyl group at the nonreducing end of substrates and inhibitors is the most significant binding mode found in previous docking studies [36] and occurs in all crystal structures of GA complexes. This structure will therefore be considered the optimal 'productive' structure for MI and will be used as reference in this study. The structures representing energetically significant docked clusters of the ten different MIs are shown in Fig. 8.

The generally low RMS deviations of the different docked structures from the reference MI structure indicate that most find similar productive docking modes. Especially close are the structures of methyl 6R-C-MI and all the MIs lacking a hydroxyl group at the nonreducing end (Fig. 8a,b). The remaining monodeoxy compounds, 2-, 3-, and especially 4-deoxy MI, deviate increasingly from the MI productive mode (Fig. 8c). This suggests that OH-4_B is important in proper binding and that OH-3_B could affect the interaction. For methyl 6S-C-MI the global minimum docked structure shows a RMS deviation of

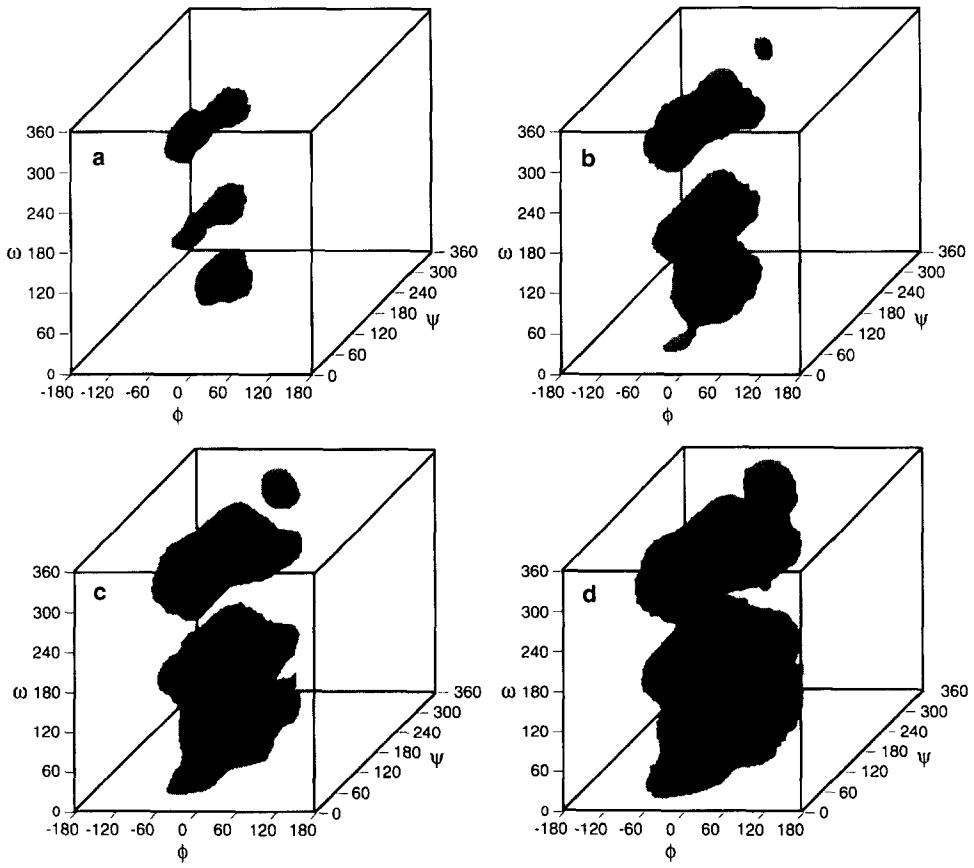

Fig. 3. MM3(92)-generated isoenergy surfaces for methyl 6R-C-MI. Panels as in Fig. 2.

0.62 Å due to both an extreme set of $\phi/\psi/\omega$ angles and an incomplete penetration of the active site due to internal and protein–substrate steric contacts.

The global minimum productive binding modes and the respective cluster averages of the different MIs, except for the methyl 6S-C-MI and 2-, 3-, and 4-deoxy MI cases, have $\phi/\psi/\omega$ angles between $-39°$ and $-14°/137°$ and $150°/-3°$ and 21°. This ground-state conformation range contrasts with the MI transition-state model where $\phi/\psi/\omega = -47°/134°/47°$, suggested recently following limited conformational exploration with GEGOP [23]. The flexibility of the three-bond glycosidic linkage allows a large set of possible conformations in the GA active site. This could explain the low rate of GA-catalyzed isomaltose hydrolysis, since not all binding modes would directly lead to catalysis. Thus, the extra step found by steady-state kinetic studies [51] could have a conformational basis.

The number of possible conformations is reduced for methyl 6R-C-MI, where the extra methyl group limits conformational space, restricting the docking results. In the first round of docking experiments (data not shown), this compound exhibited the largest energy difference between the first and second clusters and the largest number of conformers in the first cluster. The reduced number of possible conformers upon binding correlates with the low K_M of methyl 6R-C-MI [27]. In fact, the binding mode and total interaction energy are similar to those of MI, suggesting that entropic limitations could explain their different behavior in GA catalysis.

The extra methyl group in methyl 6S-C-MI is unfavorably placed for GA binding. Docking is accomplished only at the expense of the glycosidic bond torsional energy — at normal ϕ and ψ values for docked MIs, lower ω values are penalized for this compound (Fig. 7a) — and a weak interaction with active-site residues due to an incomplete penetration of the active-site pocket (Fig. 8a). Flexibility of GA active-site residues, notably that of Tyr311, which were not considered in this study, could render the binding of this compound less difficult.

In fact, according to the three-dimensional conformational maps produced by MM3(92) (Figs. 2–4), estimated energies (mostly dependent on glycosidic torsions) of the global minimum productive MI, methyl 6R-C-MI, and methyl 6S-C-MI conformers

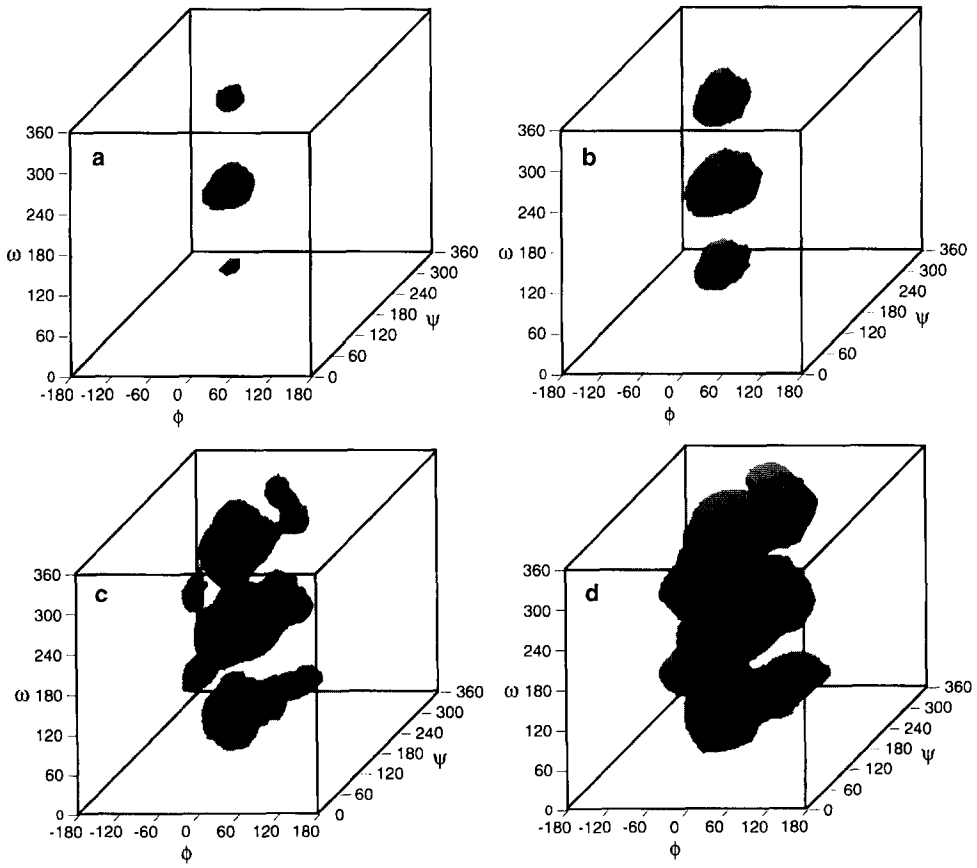

Fig. 4. MM3(92)-generated isoenergy surfaces for methyl 6S-C-MI. Panels as in Fig. 2.

are 5.7, 4.0, and 8.3 kcal/mol, respectively. Even though the conformers were found using AutoDock's simple force field, less strain is found upon docking for the best substrate, methyl 6R-C-MI, while the most was found in the worst substrate of the three [27], methyl 6S-C-MI. This result confirms that different strains on the glycosidic bond can be very important for GA hydrolysis of isomaltose analogues.

A rough estimation of the glycosidic three-bond conformational energy of the different global minimum monodeoxy MI structures can be obtained by comparing the inter-ring dihedral angles with the MI map. Energies for the series 2′-, 3′-, 4′-, and 6′-deoxy MI are 6.0, 4.5, 5.4, and 6.5 kcal/mol, respectively, while for the global minimum 2-, 3-, and 4-deoxy MIs values of 7.0, 4.4, and 6.0 are obtained, respectively. The results are, as expected, in the order of those obtained for MI but also reflect some fluctuation. However, further rationalization would require specific MM3 maps for these compounds.

Since the Lennard-Jones-based force field of AutoDock, which allows the rapid energy evaluation used in simulated annealing, is relatively unsophisticated, the calculated internal energies of the docked MIs vary significantly and show weak correlation with MM3(92) results (data not shown). This could explain why a *gt* conformer, with low internal energy, is found as the global minimum MI structure,

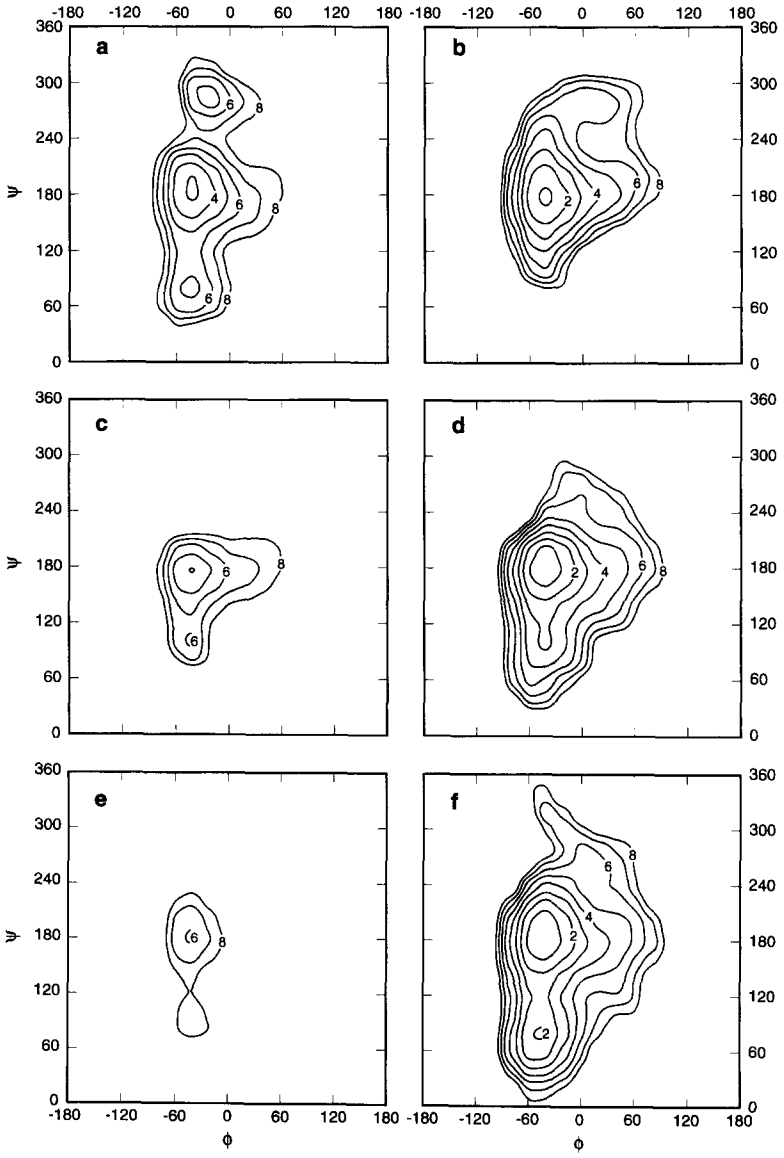

Fig. 5. MM3(92)-generated steric energy maps for MI at constant ω: (a) $\omega = 0°$, (b) $\omega = 60°$, (c) $\omega = 120°$, (d) $\omega = 180°$, (e) $\omega = 240°$, and (f) $\omega = 300°$. The ϕ, ψ planes are contoured at 1 kcal/mol increments to 8 kcal/mol above the global minimum.

while the optimal *gg* structure, which exhibits high internal energy but also has a lower intermolecular energy of interaction, appears only as the second cluster. The high internal energies exhibited by some docked results are unrealistic, and should be considered qualitatively. In most cases the differences appear to be related to orientation of the hydroxyl groups, which were allowed to rotate but which were optimized in a force field (AutoDock) that does not include torsional energy parameters. Also, even though hydroxyl groups are rotated in the same way as inter-ring bonds, AutoDock tends to optimize the latter to the detriment of the former, given their larger role in defining the binding mode. The positioning of all hydroxyl groups is then not ideal in all cases, which can cause some internal steric contacts. Given the longer interatomic distances, more confidence can be placed in the AutoDock's intermolecular component of the total energy of interaction. The fact that no solvent contribution is considered beyond a solvent screening effect included in the electrostatic calculations [45] should also affect the results. However, the structures find consistent binding modes in most cases (Fig. 8a–c).

Past studies showed good correlations between acarviosinide docking and the crystallographic data of corresponding acarbose residues [36]. In the absence of reference crystallographic structures we tried other possible correlations with experimental data. However, no significant correlations between kinetic

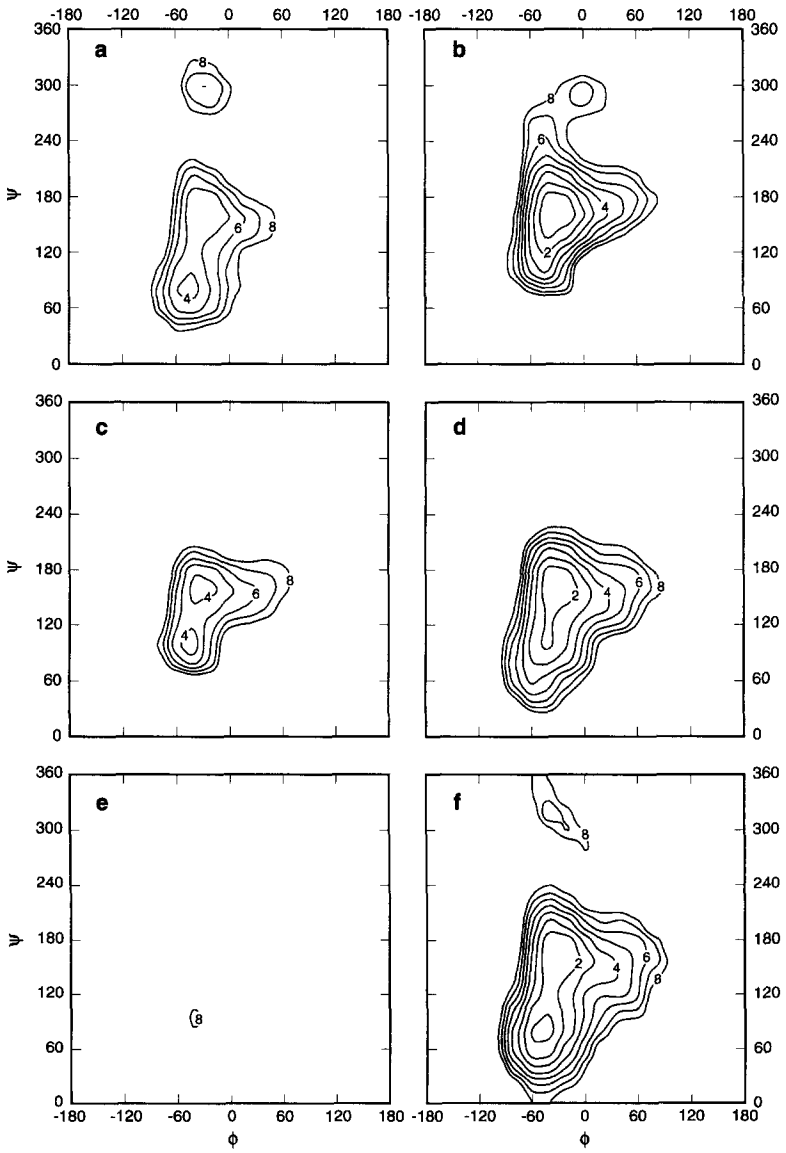

Fig. 6. MM3(92)-generated steric energy maps for methyl 6R-C-MI at constant ω: Notes as in Fig. 5 caption.

parameters [23,27] and the energy terms obtained by AutoDock or with docking structural deviations could be obtained that covered all ten substrates.

Atomic interactions in the GA active site.—Individual energy contributions to intermolecular interactions between the different MIs and the GA active site are given in Table 3. Hydrogen-atom contributions were added to those of adjacent heavy atoms. The strongest interactions of the nonreducing ends of the different MIs in the first GA subsite are made by OH-4_A and OH-6_A, the key hydroxyl groups except when they are absent in the corresponding deoxy MIs, and by C-6_A, as in the previous study [36]. The removal of these key hydroxyl groups, which strongly affects k_{cat} values of the corresponding 4′- and 6′-deoxy MIs but not their K_M values [23], still leads to regular binding modes. In addition, these compounds exhibit less negative interaction energies at the first subsite (GA-S_A in Table 3), compensating for their missing intermolecular hydrogen bonds by having stronger contacts through OH-6_A and OH-3_A, respectively.

Of all the energetic interactions at the first subsite, the weakest occurs at O-5_A in all MIs, suggesting some strain due to combined mildly unfavorable van der Waals interactions, as found for monosaccharide substrates [36]. Strain is similarly found at the glycosidic O-6_B, being major for the conformationally impaired methyl 6S-C-MI and less stringent for the global minimum 4-deoxy MI conformer, as the distances between this atom and OE1 of Glu179 equally suggest. When combined with the strong interactions

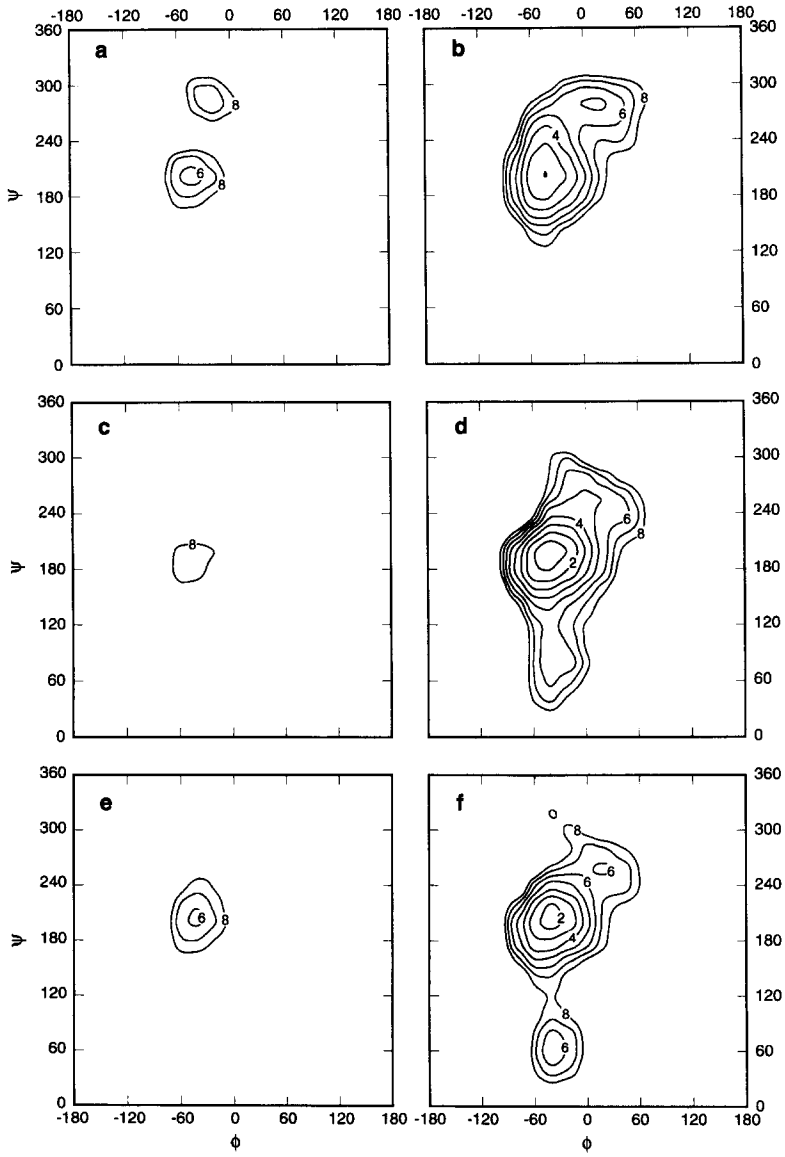

Fig. 7. MM3(92)-generated steric energy maps for methyl 6S-C-MI at constant ω: Notes as in Fig. 5 caption.

Table 1
Calculated minima for the methyl α-isomaltosides from conformational analysis

Compound	Dihedral angle (deg)			MM3 energy (kcal/mol)	Relative energy (kcal/mol)	Starting conformer
	ϕ	ψ	ω			
MI	−44.1	−172.9	−50.2	21.871	0.000	*gtrr*
	−41.5	−173.5	177.8	21.923	0.052	*gtrc*
	−43.8	−179.6	60.1	22.540	0.669	*gtcc*
	−46.9	82.1	−52.5	23.592	1.721	*gtrr*
	−44.3	100.5	175.4	24.547	2.677	*gtrr*
	−27.4	−61.1	−28.7	25.302	3.432	*gtrr*
	−23.2	−77.8	41.4	26.760	4.889	*gtcc*
Methyl 6R-C-MI	−32.4	163.7	61.4	25.872	0.000	*ggcc*
	−46.1	85.8	−48.3	26.226	0.354	*gtrr*
	−30.4	170.0	−48.6	26.772	0.901	*gtrr*
	−30.2	167.8	173.7	27.085	1.241	*gtrr*
	−43.9	102.5	172.8	27.567	1.696	*gtrr*
	−30.0	−53.4	−33.2	29.533	3.662	*gtrr*
	−8.9	−62.3	44.3	31.346	5.475	*gtrr*
Methyl 6S-C-MI	−40.8	−161.7	−179.7	24.795	0.000	*gtrc*
	−40.4	−151.4	−52.7	26.243	1.447	*gtrr*
	−44.6	−154.4	59.8	26.661	1.866	*gtcc*
	−26.3	−61.4	−30.7	29.554	4.759	*gtrr*
	−36.7	81.4	168.7	29.584	4.789	*ggcc*
	−37.6	62.8	−70.3	29.798	5.002	*gtrr*

at C-6_A and O-6_A [36], probably associated with the distortions at C-5_A found in different crystallographic studies [9], this pressure leads more easily to the oxycarbonium ion expected in the transition state of an S_N1 reaction, which is suggested by GA hydrolysis of α-D-glucopyranosyl fluoride [52].

The strongest interaction of the reducing end with the GA active site clearly occurs with OH-4_B. The removal of this hydroxyl group forces 4-deoxy MI into alternative binding modes less strained at O-6_B, leading to very different docking clusters (Table 2). The global minimum structure is represented in Fig. 8c, where the glycosidic oxygen is more than 3 Å from atom OE1 of the catalytic acid Glu179, a larger distance than the 2.6–2.7 Å interval found for most MIs (Table 3). Conformers closer to the global minimum structures of other MIs are, however, found in the third cluster (Table 2). Even though strongly affecting k_{cat}, these structures must be reasonably stable because there is a significant decrease in K_M [23]. Relatively strong interactions of OH-3_B are found in the MIs missing a nonreducing-end hydroxyl group, partially compensating for the interaction energy lost at the first subsite. Beside the strained interaction with O-6_B (except in 4-deoxy MI), weaker interaction energy values found for other atoms or groups reflect the increased distance from the protein and the unaccounted for exposure to the solvent. Interestingly, the decrease of the intermolecular energy contribution at the second subsite (GA-S_B in Table 3) of 2-, 3-, and 4-deoxy MI correlates with their RMS deviations from the reference structure and with their k_{cat}/K_M values. The critical hydroxyl group OH-4_B could then have a crucial role in catalysis, promoting strain in the glycosidic bond by imposing a less favorable conformation and steric contacts with the GA active site at O-6_B. The OH-3_B group appears to cause a milder but equally important version of this interaction. It is no coincidence that the conformations of the noncharged forms of methyl α-acarviosinide, a maltose analogue, in the GA active site are found in the saddle point between the two lowest minima [36], where conformational strain can be maximized in a stable environment.

Also at the second subsite, a strong nonpolar interaction is found for C-7_B of methyl 6R-C-MI. As with the C-6_B of acarviosinides [36], nonpolar interactions involving both Trp52 and Trp120 could have a role in the stabilizing both substrates and inhibitors. Such interactions do not occur for the corresponding methyl group in methyl 6S-C-MI, where steric contacts cause an incomplete penetration into the active-site pocket (Fig. 8a).

The overall scheme of hydrogen-bonding interactions found for ground-state MI (Fig. 8a) is similar to that recently described for the MI transition state [23],

Table 2
Redocking of methyl α-isomaltosides in the GA active site [a]

Compound	Cluster [No. of structures]	Total energy [b] (kcal/mol)	Internal energy [b] (kcal/mol)	Inter-ring dihedral angle [b]			Exo-cyclical angle		RMS deviation from ref. [b,c] (Å)
				ϕ	ψ	ω	Optimal	*gg / gt / tg*	
MI	1 [136/300]	−97.5 (−90.9)	0.50 (5.6)	−19 (−18)	132 (137)	18 (9)	*gt*	99/37/0	0.57 (0.47)
	2 [43/300]	−96.0 (−91.9)	10.2 (11.1)	−20 (−23)	146 (148)	4 (8)	*gg*	43/0/0	0.00 (0.24)
Methyl 6R-C-MI	1 [212/300]	−102.3 (−96.5)	8.0 (1.4)	−27 (−30)	137 (141)	16 (17)	*gg*	93/0/0	0.31 (0.40)
Methyl 6S-C-MI	1 [61/300]	−76.0 (−70.9)	14.8 (15.4)	−41 (−43)	127 (126)	36 (34)	*gg*	61/0/0	0.62 (0.69)
2′-Deoxy MI	1 [97/300]	−93.8 (−87.1)	7.4 (8.9)	−17 (−28)	144 (150)	5 (11)	*gg*	97/0/0	0.24 (0.37)
3′-Deoxy MI	1 [272/300]	−96.8 (−88.9)	7.1 (4.6)	−39 (−30)	148 (144)	20 (18)	*gg*	186/86/0	0.38 (0.43)
4′-Deoxy MI	1 [164/300]	−96.5 (−87.1)	1.4 (2.2)	−14 (−30)	140 (140)	−3 (21)	*gg*	161/3/0	0.19 (0.47)
6′-Deoxy MI	1 [210/400]	−96.5 (−90.5)	2.4 (2.9)	−16 (−31)	139 (141)	0 (20)			0.31 (0.54)
2-Deoxy MI	1 [46/300]	−96.9 (−91.9)	1.7 (5.4)	−14 (−4)	129 (143)	12 (−5)	*gg*	45/1/0	0.46 (0.48)
3-Deoxy MI	1 [177/400]	−97.7 (−91.8)	−0.8 (1.8)	−34 (−32)	143 (138)	43 (35)	*gg*	155/22/0	0.68 (0.64)
	2 [118/400]	−97.6 (−89.2)	−0.8 (1.3)	−21 (−28)	138 (136)	20 (24)	*gt*	2/116/0	0.52 (0.67)
4-Deoxy MI	1 [74/500]	−90.8 (−84.8)	3.8 (4.9)	4 (−6)	−162 (−117)	34 (46)	*gg*	72/2/0	2.00 (1.79)
	2 [7/500]	−88.4 (−83.9)	5.9 (4.8)	−31 (−18)	166 (124)	81 (60)	*gg*	7/0/0	1.54 (1.51)
	3 [95/500]	−87.3 (−82.8)	2.8 (4.2)	−27 (−31)	143 (141)	11 (17)	*gt*	22/73/0	0.61 (0.60)

[a] Docked structures are grouped into clusters, the best clusters being shown.
[b] Values for the optimal structure in each cluster are to the left and cluster averages are in parentheses.
[c] Using equivalent atoms of the best productive binding mode of MI following redocking.

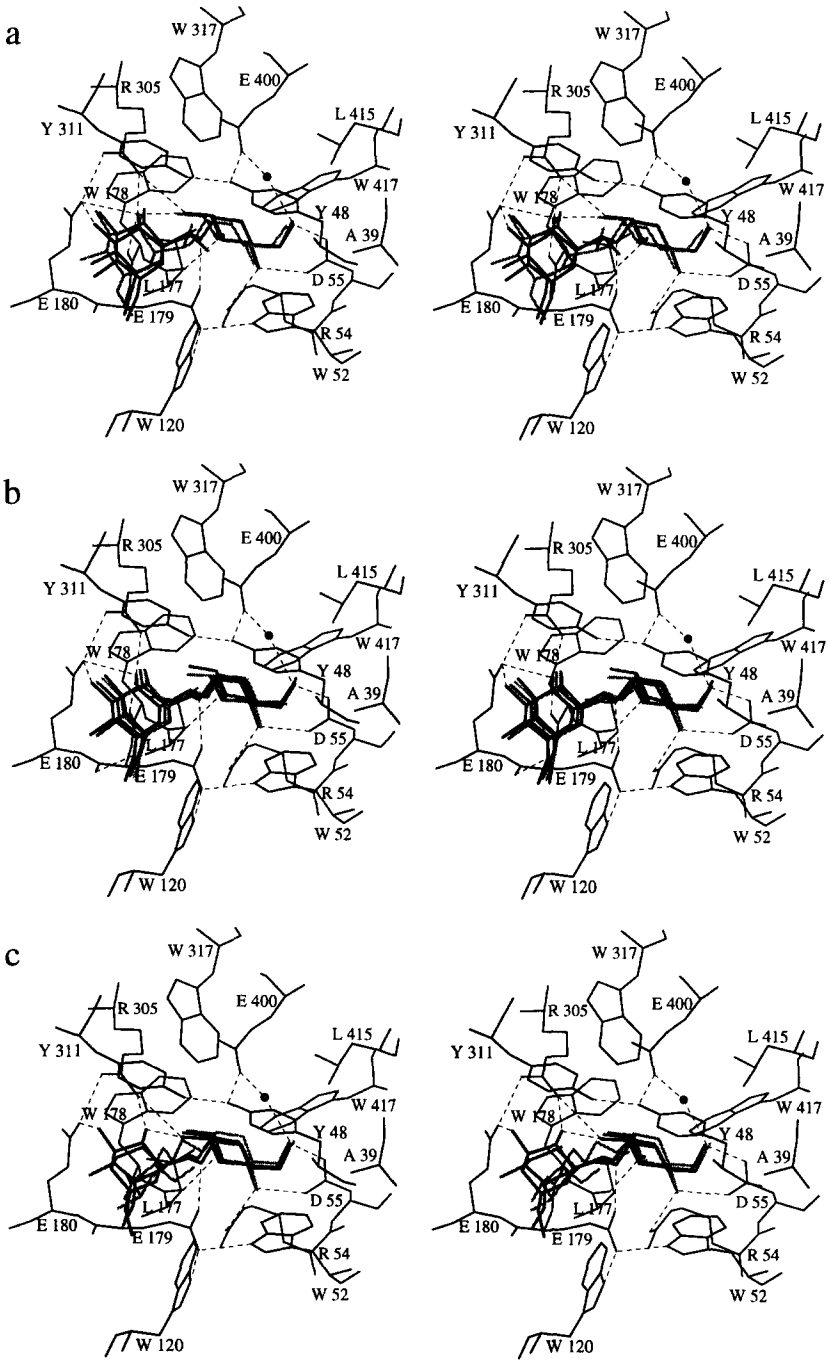

Fig. 8. Stereoscopic plots of docked structures in the GA active site. Residues surrounding the first and second subsites and the catalytic water are shown, along with hydrogen bonding between protein and substrate residues indicated by dashed lines. (a) MI (black), methyl 6R-C-MI (dark grey) and methyl 6S-C-MI (light grey); (b) 2′-deoxy-MI (black), 3′-deoxy-MI (dark grey), 4′-deoxy-MI (medium grey), and 6′-deoxy-MI (light grey); (c) 2-deoxy-MI (black), 3-deoxy-MI (dark grey) and 4-deoxy-MI (light grey). Plots were prepared with Molscript [50].

[a] GA-S_i: intermolecular energy per subsite, GA-S: total intermolecular energy per substrate, $S_{Internal}$: relative internal energy of the substrate. A: first subsite, B: second subsite, C: third subsite.
[b] Bold: Interaction with critical hydroxyl groups.
[c] Refs. [23,27].

Table 3
Atomic contributions to intermolecular energy (kcal/mol) in the interaction of the optimal structures of methyl α-isomaltosides with the GA active site [a]

Atom	MI	Methyl 6R-C-MI	Methyl 6S-C-MI	2′-Deoxy MI	3′-Deoxy MI	4′-Deoxy MI	6′-Deoxy MI	2-Deoxy MI	3-Deoxy MI	4-Deoxy MI
$C\text{-}1_A$	−4.9	−4.9	−4.6	−4.7	−5.0	0−4.9	−4.8	−4.4	−5.0	−5.2
$C\text{-}2_A$	−4.8	−5.2	−5.1	−6.4	−3.9	−4.9	−4.9	−4.9	−4.8	−3.8
$C\text{-}3_A$	−5.6	−5.7	−0.5	−5.3	−7.3	−4.5	−4.6	−4.4	−5.6	−4.9
$C\text{-}4_A$	−5.2	−5.3	−4.5	−5.0	−5.4	−6.4	−5.3	−5.1	−5.2	−5.3
$C\text{-}5_A$	−4.9	−4.9	−3.1	−4.6	−4.7	−5.3	−5.3	−5.1	−4.8	−5.2
$C\text{-}6_A$	−8.8	−8.7	−6.5	−7.5	−8.3	−9.1	−9.8	−8.6	−8.7	−8.8
$O\text{-}2_A$	−5.4	−4.8	−4.8		−5.8	−4.1	−4.8	−4.0	−4.2	−4.4
$O\text{-}3_A$	−3.6	−7.2	−4.9	−8.0		−5.8	−8.6	−5.9	−6.2	−7.8
$O\text{-}4_A$ [b]	**−9.6**	**−11.4**	**−9.8**	**−9.8**	**−11.5**		**−9.2**	**−9.6**	**−11.4**	**−10.0**
$O\text{-}5_A$	−1.9	−1.8	−1.5	−1.8	−1.9	−1.4	−1.6	−1.9	−1.9	−1.3
$O\text{-}6_A$ [b]	**−10.5**	**−5.7**	**−7.2**	**−7.5**	**−9.9**	**−10.9**		**−10.1**	**−8.9**	**−9.1**
$C\text{-}1_B$	−2.8	−2.3	−1.7	−2.4	−2.8	−2.9	−2.8	−1.9	−1.6	−2.3
$C\text{-}2_B$	−1.5	−1.6	−1.4	−1.5	−1.5	−1.5	−1.5	−1.9	−2.1	−1.5
$C\text{-}3_B$	−3.8	−3.9	−3.3	−3.7	−3.2	−3.7	−3.3	−3.7	−3.5	−3.2
$C\text{-}4_B$	−4.0	−4.0	−3.7	−3.9	−3.8	−3.9	−3.7	−3.8	−4.3	−3.8
$C\text{-}5_B$	−3.6	−3.6	−3.6	−3.9	−3.5	−3.6	−3.4	−3.5	−3.4	−3.4
$C\text{-}6_B$	−4.8	−4.0	−3.0	−4.7	−4.7	−5.1	−5.1	−4.8	−4.8	−4.8
$C\text{-}7_B$		−7.0	−3.2							
$O\text{-}2_B$	−0.8	−1.1	−0.7	−0.8	−0.6	−0.8	−0.7		−0.8	−0.7
$O\text{-}3_B$	−1.5	−2.6	−1.7	−2.5	−4.0	−4.8	−4.0	−2.8		−1.9
$O\text{-}4_B$ [b]	**−8.2**	**−6.6**	**−5.7**	**−8.1**	**−6.0**	**−5.9**	**−5.1**	**−6.3**	**−3.8**	
$O\text{-}5_B$	−1.2	−1.1	−1.0	−1.1	−1.3	−1.2	−1.2	−1.0	−0.9	−0.6
$O\text{-}6_B$	0.6	0.6	5.4	1.0	−0.0	0.3	0.4	2.2	0.2	−1.2
$C\text{-}1_C$	−7.9	−6.1	−8.3	−7.2	−7.0	−6.5	−7.6	−5.6	−3.7	−4.6
$O\text{-}1_C$	−1.4	−1.4	−1.4	−1.7	−1.9	−1.1	−1.9	−1.5	−1.2	−0.7
$GA\text{-}S_A$	−65.3	−65.6	−57.4	−60.7	−63.6	−57.4	−59.0	−63.9	−66.8	−65.8
$GA\text{-}S_B$	−31.6	−37.1	−23.7	−31.6	−31.5	−32.9	−30.4	−27.7	−25.2	−23.4
$GA\text{-}S_C$	−9.3	−7.5	−9.6	−9.0	−8.8	−7.6	−9.4	−7.1	−4.8	−5.3
GA-S	−106.2	−110.2	−90.8	−101.2	−103.9	−97.9	−98.9	−98.7	−96.8	−94.6
$S_{Internal}$	10.2	8.0	14.8	7.4	7.1	1.4	2.4	1.7	−0.8	3.8
Total	−96.0	−102.2	−76.0	−93.8	−96.8	−96.5	−96.5	−96.9	−97.7	−90.8
k_{cat} (s^{-1}) [c]	0.88	0.68	1.1	0.18	0.95	1.3×10^{-4}	1.5×10^{-4}	0.50	0.036	6.7×10^{-4}
K_M (mM) [c]	22.4–24.5	0.71	90.0	21.2	56.9	21.2	39.0	19.1	24.1	8.8
k_{cat}/K_M ($mM^{-1}\ s^{-1}$) [c]	0.039–0.042	0.96	0.012	0.0085	0.017	6.0×10^{-6}	3.9×10^{-6}	0.026	0.0015	7.6×10^{-5}
Distance $O\text{-}6_B$-Glu179 (Å)	2.65	2.66	2.48	2.58	2.74	2.72	2.71	2.56	2.69	3.09

as well as for the nonreducing end of methyl α-maltoside [12,23]. All the monodeoxy MI forms except 4-deoxy MI have binding modes similar to that of MI. The strong impact of the removal of OH-4_A and OH-6_A on hydrolysis kinetics [23,24] should then not only be attributed to the loss of important hydrogen binding forces but equally to the imbalance of forces and charges found in the active site, especially those promoting the distortions occurring at C-5_A [9] and, in the 6′-deoxy MI case, to the loss of the interaction with the catalytic water, perturbing its nucleophilic attack at C-1_A [7]. Steric contact of the glycosidic O-6_B with Glu179 is promoted by the hydrogen bonding of OH-4_B with Arg305, the backbone of Trp178, and remotely with Glu180, and to a minor degree by hydrogen bonding between OH-3_B and Glu180. These are levers to distort the nonreducing-end ring into the transition state and to perturb the bond between C-1_A and O-6_B.

In isomaltose hydrolysis, mutation of the catalytic acid and base, Glu179 and Glu400, respectively, led to complete loss of GA activity [10,11]. An equally deleterious effect on activity toward isomaltose was caused by mutations of residues Arg54 [53] and Asp55 [54], which interact with the key hydroxyl groups in the first subsite. Interestingly, while the K_M of the Asp55 → Gly mutant is identical to that of the wild-type GA in the hydrolysis of 6′-deoxy MI [23], k_{cat} for the same reaction is one order of magnitude higher in the mutant, suggesting that the presence of OH-6_A helped stabilize the catalytic water for catalysis.

At the second subsite, the conservative GA mutation Arg305 → Lys [53], affecting interaction with the key hydroxyl group OH-4_B, has in isomaltose hydrolysis the same k_{cat} value as does wild-type GA in the hydrolysis of 4-deoxy MI and of 4-*O*-methyl MI [23], while the K_M values for isomaltose hydrolysis by both wild-type and mutant GA are similar. The K_M of 4-deoxy MI hydrolysis by wild-type GA is lower than for MI hydrolysis because less strain at O-6_B can be obtained in the alternative optimal conformer of the former, while the higher K_M in 4-*O*-methyl MI hydrolysis is caused by steric contacts with the methyl group. Removal of the weaker hydrogen bond between Glu180 and OH-3_B affected k_{cat}/K_M similarly in the hydrolysis of isomaltose by the mutant Glu180 → Gln GA and of both 3-deoxy and 3-*O*-methyl MIs by wild-type GA [10,23]. Of the remaining mutants affecting the second subsite, a low K_M occurred in isomaltose hydrolysis by mutant Trp120 → Tyr GA [55]. Given the small interaction between most MIs and Trp120, it can be speculated that the catalytic acid Glu179, normally hydrogen-bonded to Trp120, is stabilized in a slightly different position in the mutant where the glycosidic O-6_B is subjected to less strain, so that isomaltose binds more easily. However, without stress at the glycosidic bond, hydrolysis would proceed slowly.

4. Conclusions

The interaction of MI and some of its substrate analogues with the GA active site has been simulated by Monte Carlo techniques with the formation in most cases of productive binding modes. Energetic discrepancies were caused by AutoDock's simplified Lennard-Jones coefficient-based force field, by the rigidity of the pyranosyl rings, and by the random nature of the approach.

Conformational mapping of methyl 6R-C-MI and methyl 6S-C-MI revealed that in these compounds the rotation around the three-bond glycosidic bond is unequally but significantly impaired, rendering the transitions between different minima more difficult. This impairment, coupled with the positioning of the extra methyl group around C-6_B, introduces dramatic differences in the allowed docking modes in the GA active site, strongly favoring the binding of methyl 6R-C-MI over that of methyl 6S-C-MI. The results agree with the kinetic parameters [27] and suggest that entropic factors, along with a lower energy penalty in the torsion of the glycosidic linkage, render methyl 6R-C-MI a better substrate than MI, and that the slower hydrolysis of methyl 6S-C-MI is due to both conformational and steric limitations.

Based on conformational studies on MI, all the monodeoxy MIs except 4-deoxy MI yielded similar binding modes upon docking. Mapping of individual atomic interactions revealed that removal of the hydroxyl groups contributing the most binding energy at each subsite correlates with the key hydroxyl groups defined by chemical mapping [23,24]. In the extreme case of 4-deoxy MI, an alternative nonproductive binding mode was found. Variation of the binding modes is linked to flexibility of the three-bond glycosidic bonds found in all the substrates.

The study also indicated which atoms of the ground-state conformer are more stressed upon binding, indicating the pressures exerted by the GA active site that lead to formation of the transition state and then to catalysis.

The use of different minima representing the possi-

ble substrate conformational states as initial structures for docking insured the exploration of significant conformational space. This study confirms that the ability of AutoDock to dock flexible substrates can effectively be used to extend the understanding of carbohydrate–protein interactions, as indicated by a previous study [36]. Further exploration of the interaction of substrates with the GA active site could improve our knowledge of its selectivity beyond what is possible by protein crystallography.

Acknowledgements

The authors gratefully acknowledge the financial support of the U.S. Department of Agriculture through the Mid-America Food Manufacturing Alliance and that of Genencor International, Inc. P.M.C. was initially supported by grant B.D./1057/90-IF of Programa CIÊNCIA, JNICT, Lisboa, Portugal. The authors are very grateful to Alexander Aleshin and Richard Honzatko for access to crystallographic data prior to public release. Raymond Lemieux is especially thanked, since without his suggestions this study would not have been conducted. All three plus David Goodsell kindly furnished manuscripts of their work before publication.

References

[1] M.M. Meagher and P.J. Reilly, *Biotechnol. Bioeng.*, 34 (1989) 689–693.
[2] Z.L. Nikolov, M.M. Meagher, and P.J. Reilly, *Biotechnol. Bioeng.*, 34 (1989) 694–704.
[3] H. El-Sayed and E. László, *Acta Aliment.*, 23 (1994) 59–70.
[4] A. Aleshin, A. Golubev, L.M. Firsov, and R.B. Honzatko, *J. Biol. Chem.*, 267 (1992) 19291–19298.
[5] E.M.S. Harris, A.E. Aleshin, L.M. Firsov, and R.B. Honzatko, *Biochemistry*, 32 (1993) 1618–1626.
[6] A.E. Aleshin, C. Hoffman, L.M. Firsov, and R.B. Honzatko, *J. Mol. Biol.*, 238 (1994) 575–591.
[7] A.E. Aleshin, L.M. Firsov, and R.B. Honzatko, *J. Biol. Chem.*, 269 (1994) 15631–15639.
[8] B. Stoffer, A.E. Aleshin, L.M. Firsov, B. Svensson, and R.B. Honzatko, *FEBS Lett.*, 358 (1995) 57–61.
[9] A.E. Aleshin, B. Stoffer, L.M. Firsov, B. Svensson, and R.B. Honzatko, *Biochemistry* 35 (1996) 8319–8328.
[10] M.R. Sierks, C. Ford, P.J. Reilly, and B. Svensson, *Protein Eng.*, 3 (1990) 193–198.
[11] T.P. Frandsen, C. Dupont, J. Lehmbeck, B. Stoffer, M.R. Sierks, R.B. Honzatko, and B. Svensson, *Biochemistry*, 33 (1994) 13808–13816.
[12] P.M. Coutinho and P.J. Reilly, *Protein Eng.*, 7 (1994) 393–400.
[13] P.M. Coutinho and P.J. Reilly, *Protein Eng.*, 7 (1994) 749–760.
[14] B. Henrissat, P.M. Coutinho, and P.J. Reilly, *Protein Eng.*, 7 (1994) 1281–1282.
[15] A.N. Savel'ev, V.R. Sergeev, and L.M. Firsov, *Biokhimiya*, 47 (1982) 390–397.
[16] M.M. Meagher, Z.L. Nikolov, and P.J. Reilly, *Biotechnol. Bioeng.*, 34 (1989) 681–688.
[17] J. Ermer, K. Rose, G. Hübner, and A. Schellenberger, *Biol. Chem. Hoppe-Seyler*, 374 (1993) 123–128.
[18] S. Cottaz, H. Driguez, and B. Svensson, *Carbohydr. Res.*, 228 (1992) 299–305.
[19] C. Apparu, H. Driguez, G. Williamson, and B. Svensson, *Carbohydr. Res.*, 277 (1995) 313–320.
[20] W. Dong, T. Jespersen, M. Bols, T. Srydstrup, and M.R. Sierks, *Biochemistry*, 35 (1996) 2788–2795.
[21] M.K. Dowd, P.J. Reilly, and A.D. French, *Biopolymers*, 34 (1994) 625–638.
[22] M.K. Dowd, A.D. French, and P.J. Reilly, *J. Carbohydr. Chem.*, 14 (1995) 589–600.
[23] R.U. Lemieux, U. Spohr, M. Bach, D.R. Cameron, T.B. Frandsen, B. Svensson, and M.M. Palcic, *Can. J. Chem.*, 74 (1996) 319–335.
[24] K. Bock, T. Skrydstrup, and S. Refn, *J. Carbohydr. Chem.*, 10 (1991) 969–980.
[25] K. Bock and H. Pedersen, *Acta Chem. Scand. B*, 41 (1987) 617–628.
[26] N. Le, Ph.D. Thesis, Univ. of Alberta, Edmonton (1990).
[27] M.M. Palcic, T. Skrydstrup, K. Bock, N. Le, and R.U. Lemieux, *Carbohydr. Res.*, 250 (1993) 87–92.
[28] M.R. Sierks, K. Bock, S. Refn, and B. Svensson, *Biochemistry*, 31 (1992) 8972–8977.
[29] M.R. Sierks and B. Svensson, *Protein Eng.*, 5 (1992) 185–188.
[30] F. Quiocho, *Annu. Rev. Biochem.*, 55 (1986) 287–315.
[31] R.U. Lemieux, *Chem. Soc. Rev.*, 18 (1989) 347–374.
[32] R.U. Lemieux and U. Spohr, *Adv. Carbohydr. Chem. Biochem.*, 50 (1994) 1–20.
[33] D.S. Goodsell and A.J. Olson, *Proteins*, 8 (1990) 195–202.
[34] D.S. Goodsell, H. Lauble, C.S. Stout and A.J. Olson, *Proteins*, 17 (1993) 1–10.
[35] D.S. Goodsell, G.M. Morris, and A.J. Olson, *J. Mol. Recog.*, 9 (1996) 1–5.
[36] P.M. Coutinho, M.K. Dowd, and P.J. Reilly, *Proteins*, (1996), in press.
[37] N.L. Allinger, Y.H. Yuh, and J.H. Lii, *J. Am. Chem. Soc.*, 111 (1989) 8551–8566.
[38] J.H. Lii and N.L. Allinger, *J. Am. Chem. Soc.*, 111 (1989) 8566–8575.
[39] N.L. Allinger, M. Rahman, and J.H. Lii, *J. Am. Chem. Soc.*, 112 (1990) 8293–8307.
[40] M.K. Dowd, P.J. Reilly, and A.D. French, *J. Comput. Chem.*, 13 (1992) 102–114.
[41] M.K. Dowd, J. Zeng, A.D. French, and P.J. Reilly, *Carbohydr. Res.*, 230 (1992) 223–244.

[42] M.K. Dowd, A.D. French, and P.J. Reilly, *Carbohydr. Res.*, 233 (1992) 15–34.
[43] M.K. Dowd, A.D. French, and P.J. Reilly, *J. Carbohydr. Chem.*, 12 (1993) 449–457.
[44] S.N. Ha, L.K. Madsen, and J.W. Brady, *Biopolymers*, 27 (1988) 1927–1952.
[45] A. De Bruyn and M. Anteunis, *Carbohydr. Res.*, 47 (1976) 311–314.
[46] R.H. Marchessault and S. Pérez, *Biopolymers*, 18 (1979) 2369–2374.
[47] Y. Nishida, H. Ohrui, and H. Meguro, *Tetrahedron Lett.*, 25 (1984) 1575–1578.
[48] J. Gasteiger and M. Marsili, *Tetrahedron*, 36 (1980) 3219–3228.
[49] E.L. Mehler and T. Solmajer, *Protein Eng.*, 4 (1991) 903–910.
[50] P.J. Kraulis, *J. Appl. Crystallogr.*, 24 (1991) 946–950.
[51] K. Olsen, B. Svensson, and U. Christensen, *Eur. J. Biochem.*, 209 (1992) 777–784.
[52] Y. Tanaka, W. Tao, J.S. Blanchard, and E.J. Hehre, *J. Biol. Chem.*, 269 (1994) 32306–32316.
[53] T.P. Frandsen, T. Christensen, B. Stoffer, J. Lehmbeck, C. Dupont, R.B. Honzatko, and B. Svensson, *Biochemistry*, 34 (1995) 10162–10169.
[54] M.R. Sierks and B. Svensson, *Biochemistry*, 32 (1993) 1113–1117.
[55] M.R. Sierks, C. Ford, P.J. Reilly, and B. Svensson, *Protein Eng.*, 2 (1989) 621–625.